[3] K. R. Britting, *Inertial Navigation System Analysis*. New York: Wiley, 1971.
[4] R. Chatila, S. Lacroix, S. Betge-Brezetz, M. Devy, and T. Simeon, "Autonomous mobile robot navigation for planet exploration—The EDEN project," in *Proc. IEEE Int. Conf. Robot. Automat.*, 1996.
[5] G. Giralt, L. Boissier, and L. Marechal, "The Iares project: Rovers for the human conquest of the moon and Mars," in *Proc. IEEE Int. Conf. Robot. Automat.*, 1996.
[6] E. Krotkov, R. Simmons, F. Cozman, and S. Koenig, "Safeguarded teleoperation for lunar rovers: From human factors to field trials," in *Proc. IEEE Int. Conf. Robot. Automat.*, 1996.
[7] P. Maybeck, *Stochastic Models, Estimation and Control*. New York: Academic, 1982, vol. 1.
[8] NOVATEL Inc., *GPSCard*, Software Version 4.437, Hardware Version 3.05, Nov. 1996.
[9] B. W. Parkinson and J. J. Spiker, Jr., *Global Positioning System: Theory and Applications*. Washington, DC: American Institute of Aeronautics and Astronautics, Inc., 1996.
[10] S. Sukkarieh, E. M. Nebot, and H. Durrant-Whyte, "Achieving integrity in an INS/GPS navigation loop for autonomous land vehicle applications," in *Proc. IEEE Int. Conf. Robot. Automat.*, May 1998.
[11] D. H. Titterton and J. L. Weston, *Strapdown Inertial Navigation Technology*. Stevenage, U.K.: Peregrinus, 1997.
[12] F. Van Diggelen, *GPS and GPS + GLONASS RTK*, in ION-GPS, Sept. 1997.
[13] R. Volpe, J. Balaram, T. Ohm, and R. Ivlev, "The rocky 7 mars rover prototype," in *Proc. IEEE Int. Conf. Robot. Automat.*, 1996.

Sliding Mode Control for Trajectory Tracking of Nonholonomic Wheeled Mobile Robots

Jung-Min Yang and Jong-Hwan Kim

***Abstract*— Nonholonomic mobile robots have constraints imposed on the motion that are not integrable, i.e., the constraints cannot be written as time derivatives of some function of the generalized coordinates. The position control of nonholonomic mobile robots has been an important class of control problems. In this paper, we propose a robust tracking control of nonholonomic wheeled mobile robots using sliding mode. The posture of a mobile robot is represented by polar coordinates and the dynamic equation of the robot is feedback-linearized by the computed-torque method. A novel sliding mode control law is proposed for asymptotically stabilizing the mobile robot to a desired trajectory. It is shown that the proposed scheme is robust to bounded external disturbances. Experimental results demonstrate the effectiveness of accurate tracking capability and the robust performance of the proposed scheme.**

***Index Terms*—Nonholonomic wheeled mobile robots, sliding mode control, trajectory tracking.**

I. Introduction

It is known that stabilization of nonholonomic wheeled mobile robots with restricted mobility to an equilibrium state is in general quite difficult. A well-known work of Brockett [1] identifies nonholonomic systems as a class of systems that cannot be stabilized via smooth state feedback. It implies that problems of controlling nonholonomic systems cannot be applied to methods of linear control theory, and they are not transformable into linear control problems. Due to both their richness and hardness, such nonlinear control problems have motivated a large number of researches involving various techniques of automatic control. Another difficulty in controlling nonholonomic mobile robots is that in the real world there are uncertainties in their modeling. Taking into account intrinsic characteristics of mobile robots such as actual vehicle dynamics, inertia and power limits of actuators and localization errors, their dynamic equations could not be described as a simplified mathematical model. A survey of recent developments in control of nonholonomic systems is described in [2]. To the authors' knowledge, the problem of dealing with model uncertainties is one of research problems for nonholonomic systems that require much attention but have yet to be extensively studied. Among previous researches, Jiang and Pomet [3], [4] applied backstepping technique to the adaptive control of nonholonomic systems with unknown parameters. A controller robust against localization errors of nonholonomic mobile robots was proposed by Hamel et al. [5], which considered the parking problem of mobile robots. In [6], a robust path-following controller for mobile robots was proposed guaranteeing exponential stability.

As an approach for robust control, sliding mode control has been applied to the trajectory control of robot manipulators [7], [8], and is recently receiving increasing attention from researches on control of nonholonomic systems with uncertainties. The advantages of using sliding mode control include fast response, good transient performance and robustness with regard to parameter variations. Bloch and Drakunov [9] proposed a sliding mode control law for stabilizing a nonholonomic system expressed in chained form, and extended their work to tracking problems [10]. Guldner and Utkin [11], [12] proposed a Lyapunov navigation function to prescribe a set of desired trajectories for navigation of mobile robots to a specified configuration. They used sliding mode control to guarantee exact tracking of trajectories made by navigation functions. Chacal and Sira-Ramirez [13] developed a sliding mode control which exploits a property named differential flatness of kinematics of mobile robots. Aguilar et al. [14] presented a path-following feedback controller with sliding mode which is robust to localization and curvature estimation errors for a car-like robot.

While the above works are mainly based on kinematic models of nonholonomic systems, models that include dynamic effects are required for other purposes, for instance, using torques as control inputs. The approaches based on dynamic models of nonholonomic systems include the work of Su and Stepanenko [15], who developed a reduced dynamic model for simultaneous independent motion and force control of nonholonomic systems. They proposed a robust control law which is a smooth realization of sliding mode control. In Shim and Kim [16], a variable structure control law was proposed with which mobile robots converge to reference trajectories with bounded errors of position and velocity.

In this paper, we propose a novel sliding mode control law for solving trajectory tracking problems of nonholonomic mobile robots. Mobile robots with the proposed control law converge to a given reference trajectory with asymptotic stability. We use dynamic models of mobile robots to describe their behaviors with bounded disturbances in system dynamics. Specifically, posture variables of mobile robots represented in *polar coordinates* are used for designing appropriate sliding surfaces which stabilize all the posture variables. By means of the computed-torque method, error dynamics of mobile

Manuscript received March 24, 1998; revised March 23, 1999. This paper was recommended for publication by Associate Editor J. Wen and Editor A. De Luca upon evaluation of the reviewers' comments.

The authors are with the Department of Electrical Engineering, Korea Advanced Institute of Science and Technology (KAIST), Taejon-shi 305-701, Korea (e-mail: yjm@vivaldi.kaist.ac.kr; johkim@vivaldi.kaist.ac.kr).

Publisher Item Identifier S 1042-296X(99)04980-0.

1042–296X/99$10.00 © 1999 IEEE

robots is linearized and a sliding mode control law is applied for stabilizing the robots to a reference trajectory and compensating for existing disturbances. While the approach for trajectory tracking of nonholonomic systems via sliding mode control was presented in the literature [10], [15], [16], our approach has the following contributions:

1) Three-dimensional (3-D) explicit control outputs are given: In our approach, three-dimensional state variables of position and orientation in polar coordinates are explicitly given as control outputs. This feature makes it easy for our approach to be applied to tracking problems of real mobile robots. In previous researches, models of nonholonomic systems should be transformed to a chained form for using the sliding mode control so that the control outputs are given as an implicit form [10], or only a subset of posture variables is available as control outputs [15].
2) Experimental verification is shown: While no empirical study on trajectory tracking of nonholonomic systems has been reported in the literature, the proposed control law is implemented on controlling a real nonholonomic wheeled mobile robot that has the dynamic model considered in this paper. Practical issues of external disturbances are addressed and results of the robust tracking control in the real world are shown.

This paper is organized as follows: In Section II, theoretic formulation of general mechanical systems with nonholonomic constraints is addressed. Kinematics and dynamics of a mobile robot considered in this paper are derived in Section III. In Section IV, disturbances in system dynamics are described and a novel sliding mode control law is proposed based on the dynamic model with a disturbance term. In Section V, experimental results on trajectory tracking problems of a nonholonomic wheeled mobile robot are presented to validate the applicability of the proposed control scheme to real systems. Also, to show the robustness property, a comparison of our results to those obtained by another sliding mode controller is provided. Finally, some concluding remarks and problems on further studies are mentioned in Section VI.

II. Mechanical Systems with Nonholonomic Constraints

Consider a mechanical system with n-dimensional generalized coordinates $\mathbf{q}$ subject to m nonholonomic independent constraints that are in the form

$$\mathbf{A}(\mathbf{q})\dot{\mathbf{q}} = \mathbf{0} \tag{1}$$

where $\mathbf{A}(\mathbf{q})$ is an $m \times n$ full-rank matrix. Let $s_1(\mathbf{q}), \ldots, s_{n-m}(\mathbf{q})$ be a set of smooth and linearly independent vector fields in $\mathcal{N}(\mathbf{A})$, the null space of $\mathbf{A}(\mathbf{q})$, i.e.,

$$\mathbf{A}(\mathbf{q})s_i(\mathbf{q}) = \mathbf{0}, \quad i = 1, \ldots, n-m.$$

Let $\mathbf{S}(\mathbf{q}) = [s_1(\mathbf{q}) \cdots s_{n-m}(\mathbf{q})]$ be the full-rank matrix made up of these vectors such that

$$\mathbf{A}(\mathbf{q})\mathbf{S}(\mathbf{q}) = \mathbf{0} \tag{2}$$

and $\boldsymbol{\Delta}$ be the distribution spanned by these vector fields as

$$\boldsymbol{\Delta} = \operatorname{span}\{s_1(\mathbf{q}), \ldots, s_{n-m}(\mathbf{q})\},$$

then follows $\dot{\mathbf{q}} \in \boldsymbol{\Delta}$.

We are now concerned with the dynamic equation of a mechanical system with nonholonomic constraints (1), which is described by Euler-Lagrangian formulation [17], [18] as

$$\mathbf{M}(\mathbf{q})\ddot{\mathbf{q}} + \mathbf{V}(\mathbf{q}, \dot{\mathbf{q}}) = \mathbf{E}(\mathbf{q})\boldsymbol{\tau} - \mathbf{A}^T(\mathbf{q})\boldsymbol{\lambda} \tag{3}$$

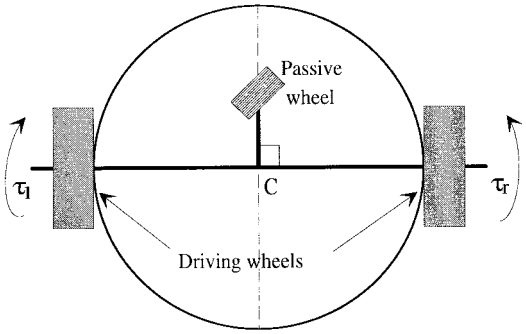

Fig. 1. Top view of the mobile robot.

where $\mathbf{M}(\mathbf{q})$ is the $n \times n$ inertia matrix, $\mathbf{V}(\mathbf{q}, \dot{\mathbf{q}})$ is the centripetal and Coriolis force term, $\mathbf{E}(\mathbf{q})$ is the $n \times r$ full-rank input transformation matrix, $\boldsymbol{\tau}$ is the r-dimensional control input vector, $\mathbf{A}(\mathbf{q})$ is the $m \times n$ Jacobian matrix, which is identical to the maxtix in (1) in the case of nonholonomic systems, and $\boldsymbol{\lambda}$ is the m-vector of constraint forces. For simplicity of analysis, we assume $r = n - m$ in this paper.

(1) and (2) imply the existence of an $(n-m)$-dimensional velocity vector $\mathbf{z} = [z_1, \ldots, z_{n-m}]^T$ such that

$$\dot{\mathbf{q}} = \mathbf{S}(\mathbf{q})\mathbf{z}. \tag{4}$$

It should be noted that $\mathbf{z}$ represents internal states so that $(\mathbf{q}, \mathbf{z})$ is sufficient to describe the constraint motion. Differentiating (4), we obtain

$$\ddot{\mathbf{q}} = \mathbf{S}\dot{\mathbf{z}} + \dot{\mathbf{S}}\mathbf{z}. \tag{5}$$

Substituting the expression for $\ddot{\mathbf{q}}$ into (3) and premultiplying by $\mathbf{S}^T$, we have

$$\mathbf{S}^T(\mathbf{M}\mathbf{S}\dot{\mathbf{z}} + \mathbf{M}\dot{\mathbf{S}}\mathbf{z} + \mathbf{V}) = \mathbf{S}^T\mathbf{E}\boldsymbol{\tau}. \tag{6}$$

Note that since $\mathbf{S} \in \mathcal{N}(\mathbf{A})$, $\mathbf{S}^T\mathbf{A}^T\boldsymbol{\lambda}$ vanishes in this equation. (6) is suitable for control purposes, because nonholonomic constraints (1) are embedded into this dynamic equation.

Multiplying by $(\mathbf{S}^T\mathbf{E})^{-1}$, (6) is reduced to

$$\mathbf{H}(\mathbf{q})\dot{\mathbf{z}} + \mathbf{G}(\mathbf{q}, \mathbf{z}) = \boldsymbol{\tau} \tag{7}$$

where $\mathbf{H}(\mathbf{q}) = (\mathbf{S}^T\mathbf{E})^{-1}\mathbf{S}^T\mathbf{M}\mathbf{S}$ is the $(n-m) \times (n-m)$ matrix, $\mathbf{G}(\mathbf{q}, \mathbf{z}) = (\mathbf{S}^T\mathbf{E})^{-1}\mathbf{S}^T(\mathbf{M}\dot{\mathbf{S}}\mathbf{z} + \mathbf{V})$ is the $(n-m) \times m$ matrix and $\boldsymbol{\tau} \in R^{(n-m)\times m}$ is the input torque vector. If the system is a wheeled mobile robot, the torque vector is applied to driving wheels.

III. Modeling of Mobile Robot

The mobile robot considered here is of unicycle type, shown in Fig. 1. The robot body is of symmetric shape and the center of mass is at the geometric center C of the body. It has two driving wheels fixed to the axis that passes through C and one passive centered orientable wheel. The two fixed wheels are controlled independently by motors, and the passive wheel prevents the robot from tipping over as it moves on a plane. In this paper, we assume that the motion of passive wheel can be ignored in dynamics of the mobile robot.

Fig. 2 shows the posture of the robot represented in the world X-Y coordinates and polar coordinates with the assumption that their origins are identical. The local coordinate system X_0-Y_0 is fixed to the robot with C as the origin. (x_c, y_c) is the position of the geometric center C in the world X-Y coordinates and θ_c is the angle between the X-axis and X_0-axis representing the heading direction. (x_c, y_c) can be also expressed as (ρ_c, ϕ_c) in polar coordinates. v_c denotes the linear velocity of the robot in the direction of X_0-axis and ω_c the angular velocity.

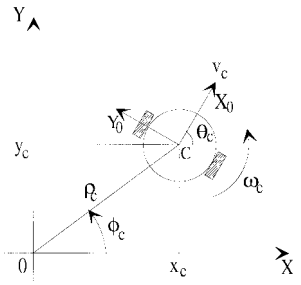

Fig. 2. Coordinates of the mobile robot.

As we are concerned with the posture of the robot, $\mathbf{q}$ is defined as

$$\mathbf{q} = [x_c, y_c, \theta_c]^T \quad \text{or} \quad [\rho_c, \phi_c, \theta_c]^T.$$

The mobile robot has the following nonholonomic constraint that the driving wheels *purely roll* and *do not slip*:

$$\dot{y}_c \cos\theta_c - \dot{x}_c \sin\theta_c = 0.$$

For $n = 3$ and $m = 1$, $\mathbf{z}$ becomes two-dimensional. We choose v_c and ω_c as the internal state variables such that

$$\mathbf{z} = [v_c, \omega_c]^T.$$

Then, (4) can be written as

$$\begin{pmatrix} \dot{x}_c \\ \dot{y}_c \\ \dot{\theta}_c \end{pmatrix} = \begin{pmatrix} \cos\theta_c & 0 \\ \sin\theta_c & 0 \\ 0 & 1 \end{pmatrix} \begin{pmatrix} v_c \\ \omega_c \end{pmatrix} \tag{8}$$

From (8) and the property of $\rho_c = \sqrt{x_c^2 + y_c^2}$ and $\phi_c = \tan^{-1}(\frac{y_c}{x_c})$, $\dot{\mathbf{q}}$ is derived in polar coordinates as follows:

$$\dot{\mathbf{q}} = \begin{pmatrix} \dot{\rho}_c \\ \dot{\phi}_c \\ \dot{\theta}_c \end{pmatrix} = \begin{pmatrix} v_c \cos(\phi_c - \theta_c) \\ -\frac{v_c}{\rho_c} \sin(\phi_c - \theta_c) \\ \omega_c \end{pmatrix} \tag{9}$$

which corresponds to Eq. (4), where

$$\mathbf{S}(\mathbf{q}) = \begin{pmatrix} \cos(\phi_c - \theta_c) & 0 \\ -\frac{1}{\rho_c} \sin(\phi_c - \theta_c) & 0 \\ 0 & 1 \end{pmatrix}$$

Instead of using the basic kinematic equation (8) derived in Cartesian coordinates, polar coordinates (9) shall be used in this work. As will be shown later, the kinematic equation in polar coordinates is suitable for easily designing appropriate sliding surfaces which decouple posture variables in a stabilizing way. For an example of using polar coordinates for control of nonholonomic mobile robots, the reader is referred to [19].

IV. Sliding Mode Controller

A. Problem Statement

It is supposed that a feasible desired trajectory for the mobile robot is pre-specified by an open-loop path planner. The problem is to design a robust controller so that the mobile robot converges to the desired trajectory. As was mentioned in the introduction, three-dimensional position and orientation variables are defined as a reference trajectory in polar coordinates:

$$\mathbf{q}_r = [\rho_r(t), \phi_r(t), \theta_r(t)]^T$$

where $\rho_r(t)$, $\phi_r(t)$ and $\theta_r(t)$ are piecewise smooth and time-varying functions. Since posture variables are independent with each other, it is not necessary that $\mathbf{q}_r$ should be given as a *closed-form* like

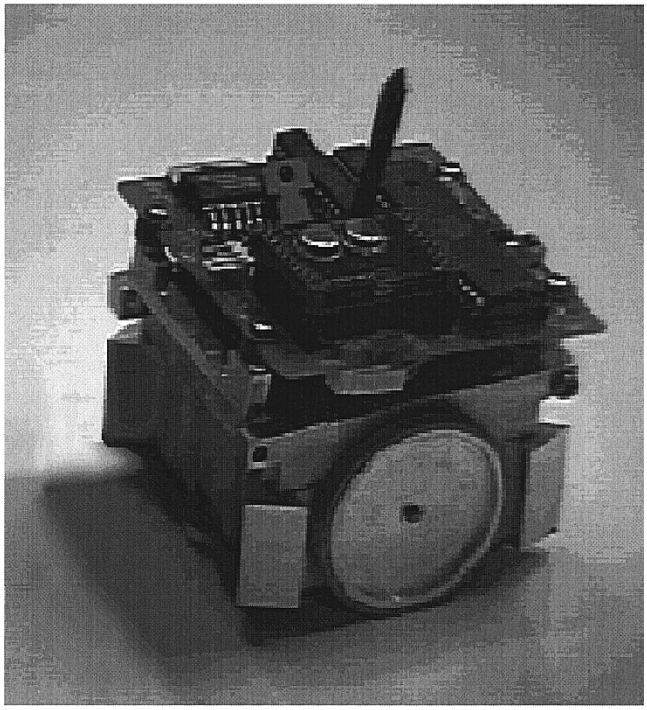

Fig. 3. MIRO robot.

$\rho_r = \psi(\phi_r)$, where $\psi(\phi_r)$ is a closed-form function of ϕ_r. $\mathbf{z}_r = [v_r(t), \omega_r(t)]^T$ is defined to be the velocity vector derived from $\mathbf{q}_r$.

Practical robotic systems have inherent system perturbations such as parameter uncertainties and external disturbances such as static friction, noise in control signals, etc. In this paper, the behavior of the mobile robot in the presence of external disturbances is considered. Let us denote the disturbances as a vector $\boldsymbol{\tau}_d \in R^{2\times 1}$. The real dynamic equation of the mobile robot with the disturbance term is represented as follows:

$$\mathbf{H}(\mathbf{q})\dot{\mathbf{z}} + \mathbf{G}(\mathbf{q}, \mathbf{z}) + \boldsymbol{\tau}_d = \boldsymbol{\tau} \tag{10}$$

where $\boldsymbol{\tau} = [\tau_l, \tau_r]^T$ is the torque vector applied to the left and right driving wheels. It is assumed that the disturbance vector can be expressed as a multiplier of matrix $\mathbf{H}(\mathbf{q})$, or it satisfies the *uncertainty matching condition*, and has a known boundary:

$$\boldsymbol{\tau}_d = \mathbf{H}(\mathbf{q})\mathbf{f},$$
$$\mathbf{f} = [f_1, f_2]^T, \quad |f_1| \le f_{m_1}, \quad |f_2| \le f_{m_2}$$

where f_{m_1} and f_{m_2} are upper bounds of disturbances. Note that, if external disturbances are bounded, the matching condition is generally satisfied since $\boldsymbol{\tau}_d = \mathbf{H}(\mathbf{H}^{-1}\boldsymbol{\tau}_d)$ and the inverse of the inertia matrix $\mathbf{H}^{-1}$ is bounded [18].

Before designing the sliding mode, the following assumptions on trajectories of the robot are given.

1) Without loss of generality, the range of the angular variables of the robot is set to be between $-\pi$ and π:
$$-\pi < \phi_r, \phi_c, \theta_r, \theta_c \le \pi.$$
2) Both the reference trajectory and the real trajectory do not cross the origin of the world coordinates after starting over the initial position. Also, the initial position of the reference trajectory is always set to be the origin:
$$\begin{aligned} \rho_r(t) &= 0, \quad t = 0 \\ \rho_r(t) &> 0, \quad t > 0 \\ |\rho_c(t)| &> \rho_f, \quad t > 0 \end{aligned} \tag{11}$$

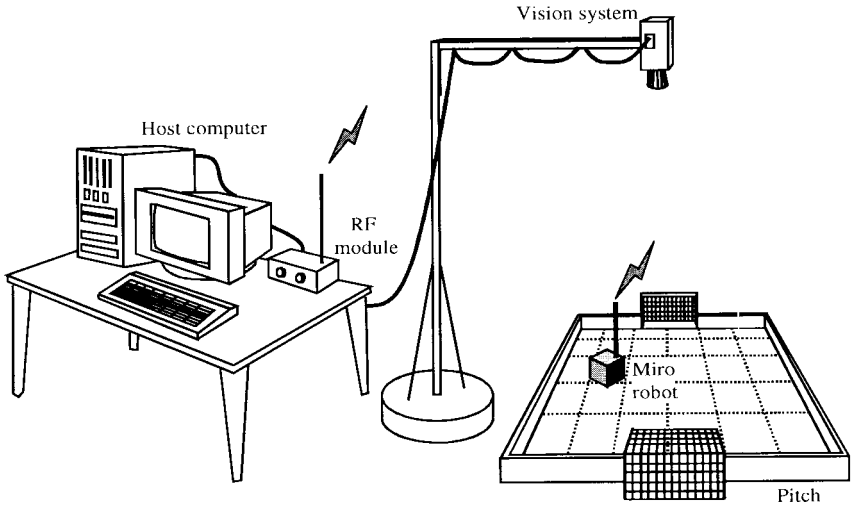

Fig. 4. Overview of the robot system.

where $\rho_f > 0$ is the upper bound of the measurement error in position. ρ_f will be nonzero if there exists inaccuracy of sensor outputs in localizing the robot.

3) The heading angle of the robot and the angle coordinate cannot be perpendicular with each other:

$$\left|\,|\phi_c(t) - \theta_c(t)| - (2m+1)\frac{\pi}{2}\right| \geq \alpha, \quad \forall t \tag{12}$$

where $m = 0$ or 1 and α is a positive constant.

The third condition in (11) indicates that when a nonzero measurement error exists, the actual trajectory of the mobile robot should not be within the vicinity of the origin made by the measurement error bound. Assumption 3) implies that the mobile robot should not have a posture whose heading direction is tangential of any circle drawn around the origin of the world coordinates.

Let us define the error of the robot posture in polar coordinates as

$$\begin{aligned}\rho_e &= \rho_c - \rho_r \\ \phi_e &= \phi_c - \phi_r \\ \theta_e &= \theta_c - \theta_r.\end{aligned}$$

B. Design of Sliding Mode

From the dynamic equations (7) and (9), we can see that the position variables ρ_c and ϕ_c are dependent on the two internal state variables v_c and ω_c, but θ_c is dependent only on ω_c. As a matter of fact, from the inherent property of mobile robots, the position and heading direction are determined by the linear and angular velocity, respectively. If we use the conventional sliding surfaces which decouples state variables according to control inputs, a sliding surface controlled by ω_c should be

$$s = \dot{\theta}_e + \gamma\theta_e$$

where $\dot{\theta}_e = \omega_c - \dot{\theta}_r$ and $\gamma > 0$. However, ρ_e and ϕ_e are unaffected by ω_c in the controlled system and consequently unable to converge to zero simultaneously by the remaining control input v_c. To solve the problem, we propose a new design of sliding surfaces in the frame of polar coordinates such that angular variables θ_e and ϕ_e are internally coupled with each other in a sliding surface leading to convergence of both variables. Let us define the vector of sliding surfaces $\mathbf{s} = [s_1, s_2]^T$ as

$$\begin{aligned}s_1 &= \dot{\rho}_e + \gamma_1\rho_e \\ s_2 &= \dot{\theta}_e + \gamma_2\theta_e + \mathrm{sgn}(\theta_e)|\phi_e|\end{aligned} \tag{13}$$

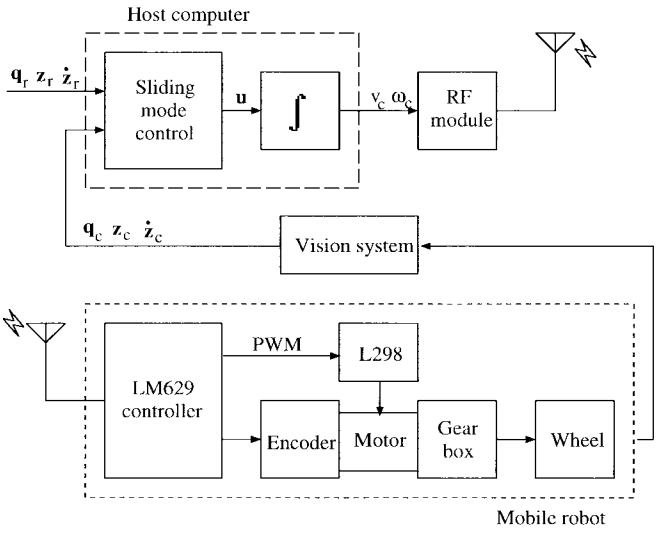

Fig. 5. Schematic diagram of the robot control system.

where γ_1 and γ_2 are positive constant parameters and $\mathrm{sgn}(\cdot)$ is the sign function.

Proposition 1: If the sliding surfaces (13) are asymptotically stable, ρ_e, ϕ_e and θ_e converge asymptotically to zeros.

Proof: If s_1 converges to zero, trivially ρ_e converges to zero. If s_2 converges to zero, in steady-state it becomes $\dot{\theta}_e = -\gamma_2\theta_e - \mathrm{sgn}(\theta_e)|\phi_e|$. Since $|\phi_e|$ is always bounded, the following relationship between θ_e and $\dot{\theta}_e$ holds:

$$\begin{aligned}\theta_e > 0 &\Rightarrow \dot{\theta}_e < 0, \\ \theta_e < 0 &\Rightarrow \dot{\theta}_e > 0.\end{aligned}$$

Therefore, the equilibrium state of θ_e is asymptotically stable. Finally, it can be known from s_2 that convergence of θ_e and $\dot{\theta}_e$ leads to convergence of $|\phi_e|$ to zero. □

As a feedback-linearization method, the control input is defined by the computed-torque method [18] as

$$\boldsymbol{\tau} = \mathbf{H}(\mathbf{q})\dot{\mathbf{z}}_r + \mathbf{G}(\mathbf{q}, \mathbf{z}) + \mathbf{H}(\mathbf{q})\mathbf{u} \tag{14}$$

where $\mathbf{u} \equiv [u_1, u_2]^T$ is a control law which determines error dynamics. Applying the proposed control law (14), the dynamic equation (10) reduces to

$$\dot{\mathbf{z}} + \mathbf{f} = \dot{\mathbf{z}}_r + \mathbf{u}. \tag{15}$$

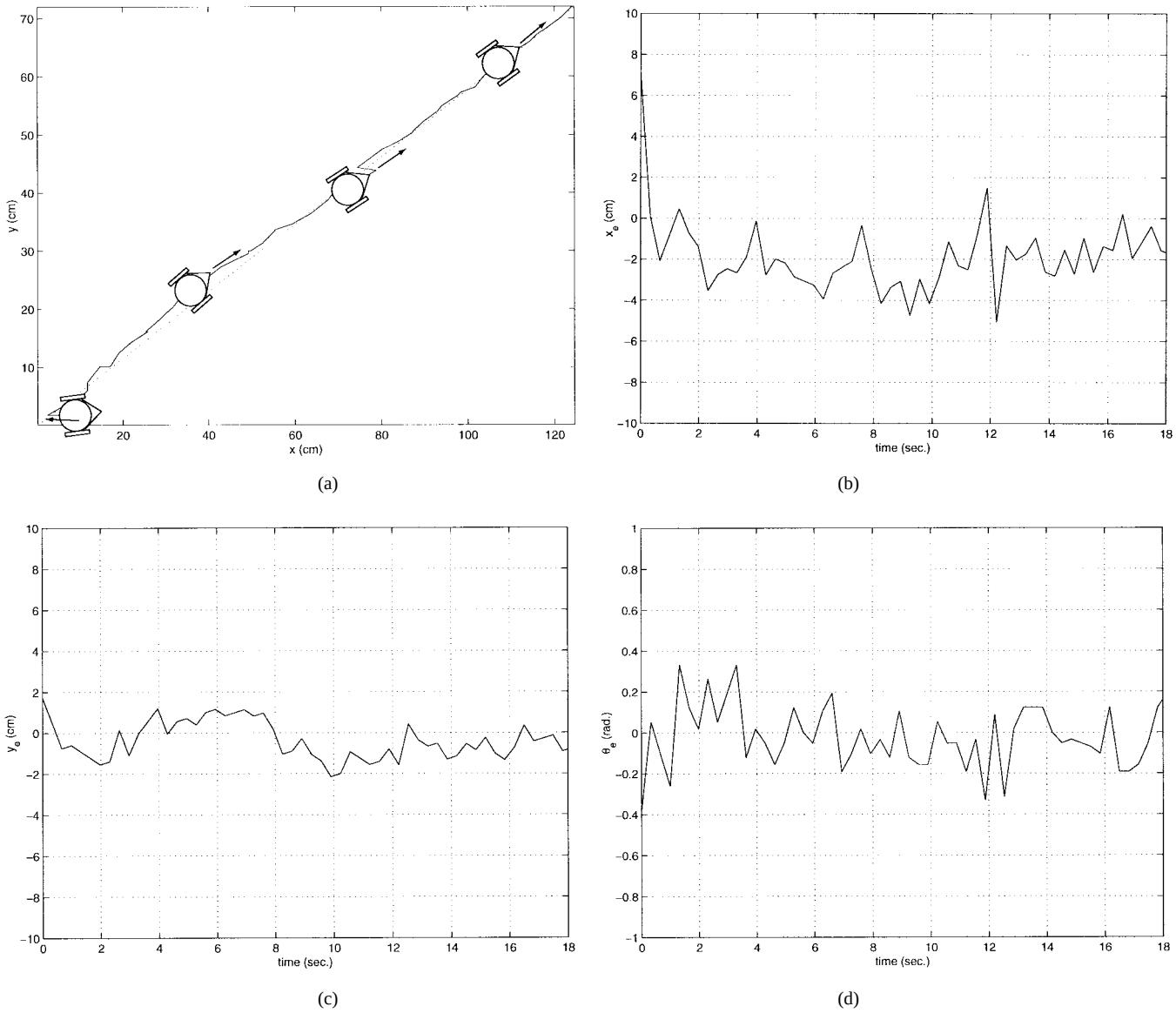

Fig. 6. Straight-line motion using the proposed controllerwith initial errors of (7.09 cm, 1.72 cm, -0.38 radian): (a) x-y plot (dotted line is the reference trajectory), (b) x_e, (c) y_e, and (d) θ_e.

In the following theorem, we propose the control law $\mathbf{u}$ which stabilizes the sliding surface vector $\mathbf{s}$. Before postulating the theorem, let us introduce the following functions that will be used in the theorem:

$$R(\mathbf{q},\mathbf{z}) = \frac{v_c^2}{\rho_c}\sin^2(\phi_c-\theta_c) + v_c\omega_c\sin(\phi_c-\theta_c),$$
$$R(\mathbf{q}_r,\mathbf{z}_r) = \frac{v_r^2}{\rho_r}\sin^2(\phi_r-\theta_r) + v_r\omega_r\sin(\phi_r-\theta_r).$$

Note that $R(\mathbf{q},\mathbf{z})$ and $R(\mathbf{q}_r,\mathbf{z}_r)$ are well-defined from assumption 2).

Theorem 1: Let us define a robust control law as

$$u_1 = \frac{1}{\cos(\phi_c-\theta_c)}\{-Q_1 s_1 - P_1\,\mathrm{sgn}(s_1) - \gamma_1\dot{\rho}_e + \dot{v}_r\cos(\phi_r-\theta_r) + R(\mathbf{q}_r,\mathbf{z}_r) - R(\mathbf{q},\mathbf{z})\} - \dot{v}_r, \quad (16)$$
$$u_2 = -Q_2 s_2 - P_2\,\mathrm{sgn}(s_2) - \gamma_2\dot{\theta}_e - \mathrm{sgn}(\theta_e)\frac{d}{dt}|\phi_e|$$

where Q_i and P_i, $i=1,2$, are constant positive values. It should be noted that $\cos(\phi_c-\theta_c)\neq 0$ from assumption 3). The above control law stabilizes the sliding surfaces (13) if the following conditions hold:

$$Q_i \geq 0 \quad \text{and} \quad P_i \geq f_{m_i}, \quad i=1,2. \quad (17)$$

Proof: The second derivative of ρ_c is calculated as

$$\begin{aligned}\ddot{\rho}_c &= (v_c\cos(\phi_c-\theta_c))' \\ &= \dot{v}_c\cos(\phi_c-\theta_c) + \frac{v_c^2}{\rho_c}\sin^2(\phi_c-\theta_c) + v_c\omega_c\sin(\phi_c-\theta_c) \\ &= \dot{v}_c\cos(\phi_c-\theta_c) + R(\mathbf{q},\mathbf{z}).\end{aligned}$$

Therefore, $\ddot{\rho}_e$ is expressed as

$$\begin{aligned}\ddot{\rho}_e &= \ddot{\rho}_c - \ddot{\rho}_r \\ &= \dot{v}_c\cos(\phi_c-\theta_c) + R(\mathbf{q},\mathbf{z}) - \dot{v}_r\cos(\phi_r-\theta_r) - R(\mathbf{q}_r,\mathbf{z}_r).\end{aligned} \quad (18)$$

Substituting the expression for $\ddot{\rho}_e$ into u_1, we have

$$u_1 = \frac{1}{\cos(\phi_c-\theta_c)}(-Q_1 s_1 - P_1\,\mathrm{sgn}(s_1) - \gamma_1\dot{\rho}_e - \ddot{\rho}_e) + \dot{v}_c - \dot{v}_r. \quad (19)$$

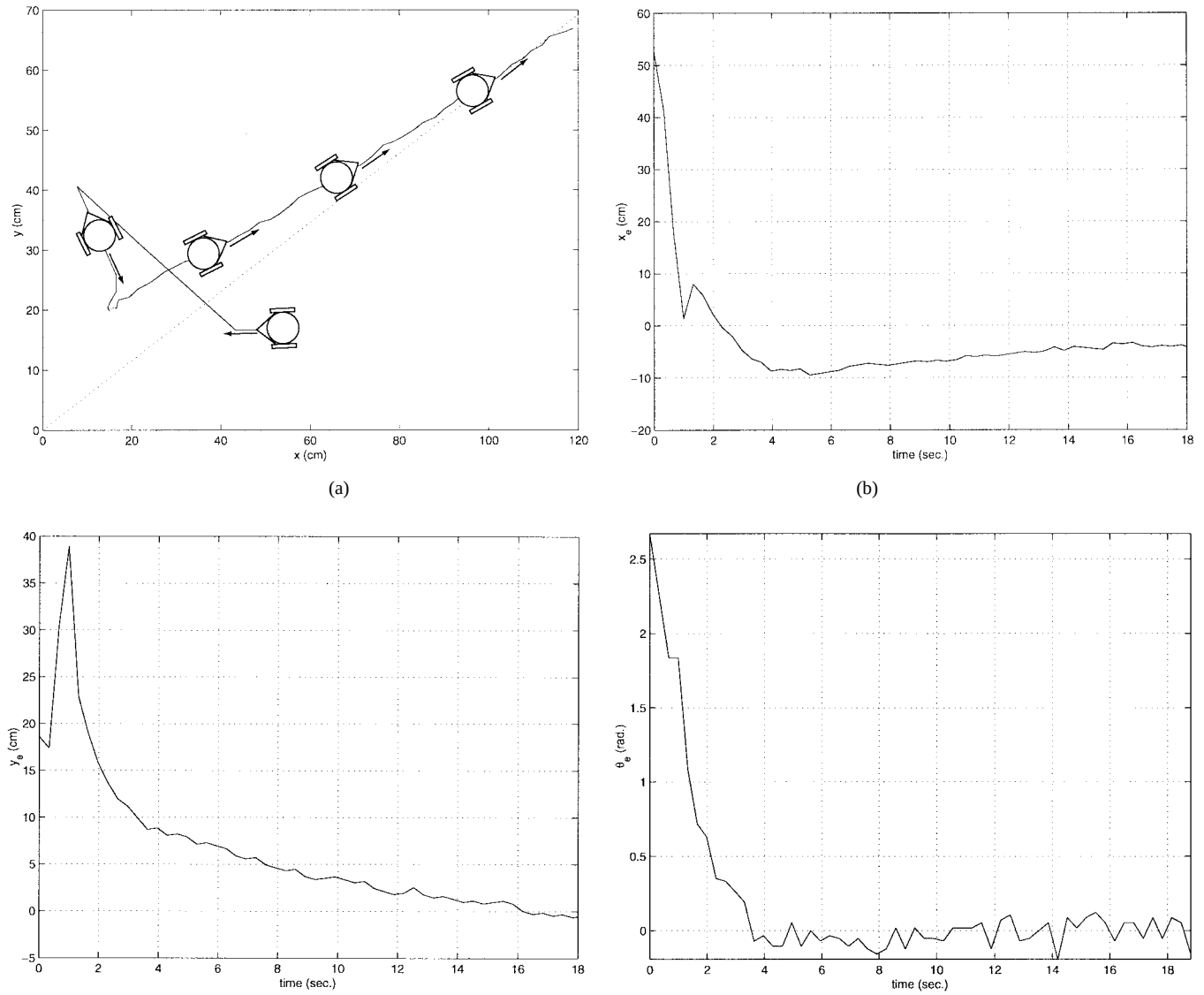

Fig. 7. Straight-line motion using the proposed controller with initial errors of (52.58 cm, 16.62 cm, -3.09 radian): (a) x-y plot (dotted line is the reference trajectory), (b) x_e, (c) y_e and (d) θ_e.

The first law of (15) is

$$\dot{v}_c + f_1 = \dot{v}_r + u_1. \tag{20}$$

From (19) and (20),

$$\ddot{\rho}_e = -Q_1 s_1 - P_1 \operatorname{sgn}(s_1) - \gamma_1 \dot{\rho}_e - f_1 \cos(\phi_c - \theta_c). \tag{21}$$

Similarly, $\ddot{\theta}_e$ is expressed as

$$\ddot{\theta}_e = -Q_2 s_2 - P_2 \operatorname{sgn}(s_2) - \gamma_2 \dot{\theta}_e - \operatorname{sgn}(\theta_e) \frac{d}{dt}|\phi_e| - f_2. \tag{22}$$

Define $V = \frac{1}{2}\mathbf{s}^T\mathbf{s}$ as a Lyapunov function candidate. Then, from (21) and (22), $\dot{V}$ is derived as

$$\begin{aligned}\dot{V} &= s_1\dot{s}_1 + s_2\dot{s}_2 \\ &= s_1(\ddot{\rho}_e + \gamma_1\dot{\rho}_e) + s_2\left(\ddot{\theta}_e + \gamma_2\dot{\theta}_e + \operatorname{sgn}(\theta_e)\frac{d}{dt}|\phi_e|\right) \\ &= s_1(-Q_1 s_1 - P_1\operatorname{sgn}(s_1) - f_1\cos(\phi_c - \theta_c)) \\ &\quad + s_2(-Q_2 s_2 - P_2\operatorname{sgn}(s_2) - f_2) \\ &= -\mathbf{s}^T Q \mathbf{s} - (P_1|s_1| + f_1 s_1 \cos(\phi_c - \theta_c)) - (P_2|s_2| + f_2 s_2).\end{aligned} \tag{23}$$

For $\dot{V}$ to be negative semi-definite, it is sufficient to choose Q_i and P_i such that $Q_i \geq 0, P_i \geq f_{m_i}, i = 1, 2$. □

Remarks:

1) The form of the proposed control law (16) is similar to that of the reaching law method [20]. Specifically, predividing of $\cos(\phi_c - \theta_c)$ is included in u_1 for deriving the acceleration term of ρ_e. While boundedness of u_1 is guaranteed by (12), u_1 might be large if α in assumption 3) is near to zero. High input values may cause unfavorable effects such as actuator saturation, energy consumption, etc. But such a drawback is compensated by the property that using u_1 reduces the effect of disturbance f_1. As we can see from (23), the real boundary of disturbance f_1 which should be eliminated by the sliding mode control law decreases as does the value of $\cos(\phi_c - \theta_c)$.
2) Because of the switching function $\operatorname{sgn}(\theta_e)|\phi_e|$, the behavior of the sliding surface s_2 is highly affected by θ_e. Suppose θ_e fluctuates from negative to positive around zero at some instant. Then Δs_2 is affected by the change of $|\phi_e|$. This characteristic might be a cause for chattering. Conversely, the

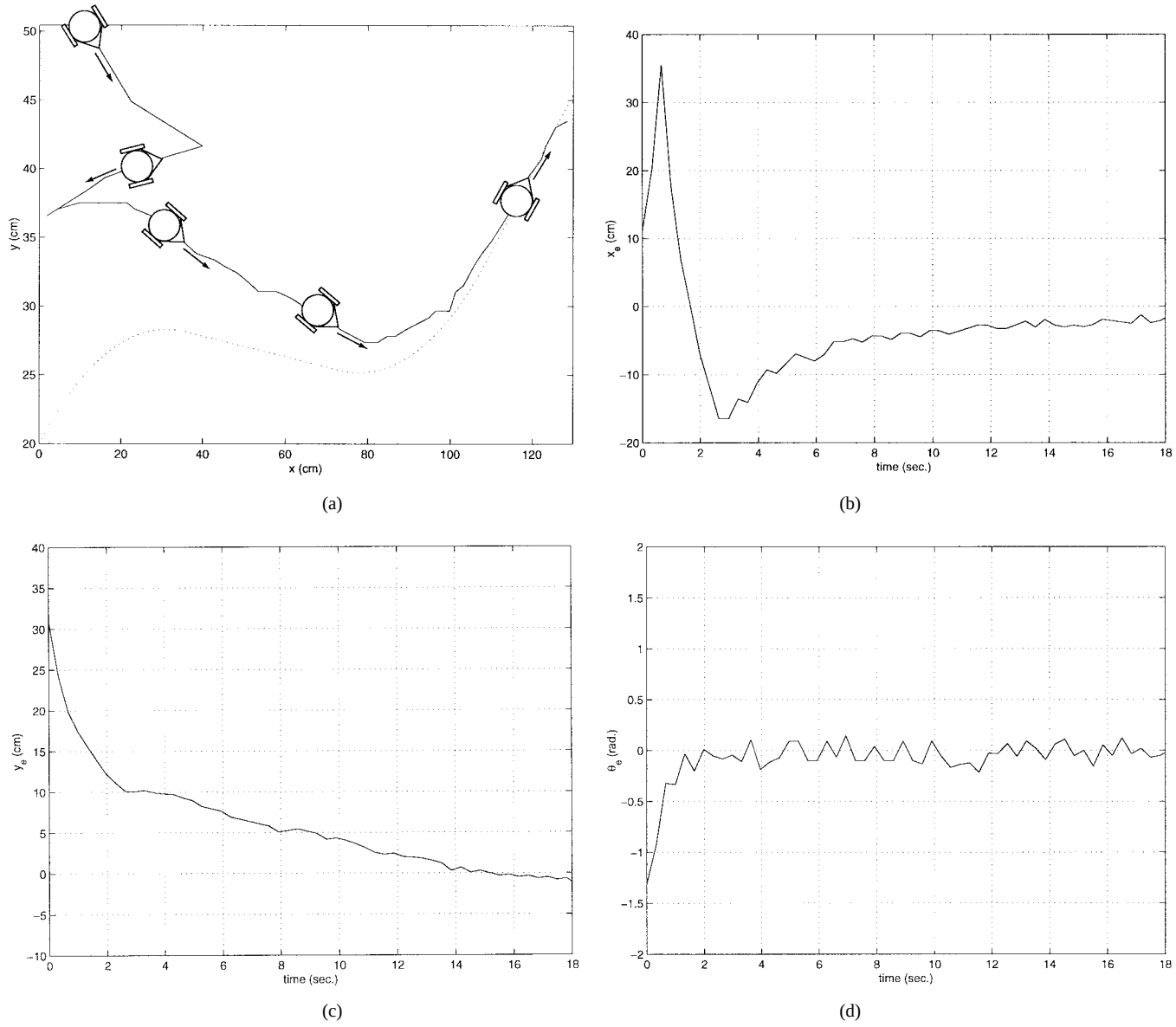

Fig. 8. Curve motion using the proposed controller with initial errors of (11.20 cm, 28.92 cm, -1.31 radian): (a) x-y plot (dotted line is the reference trajectory), (b) x_e, (c) y_e and (d) θ_e.

chattering behavior of θ_e produced by parameter variations or disturbances may lead to oscillation of ϕ_e in s_2. For design of more stable sliding surfaces and overcoming chattering, it will be necessary to use a continuous function instead of $\mathrm{sgn}(\cdot)$ such as, for instance, the saturation function.

V. Experiments

A. Experimental Setup

To demonstrate the effectiveness and applicability of the proposed method, a real-time implementation of the control strategy was developed for a mobile robot named MIRO made for the purpose of playing robot-soccer games [21], [22]. Fig. 3 shows the feature of the mobile robot of which size is 7.5 cm $\times$ 7.5 cm $\times$ 7.5 cm. It has the same structure as in Fig. 1, with two driving wheels and one passive centered orientable wheel. Specifically, in the MIRO robot a *rolling-ball* is attached as the substitution of the passive wheel. The use of the rolling-ball would be desirable because it is omnidirectional so that its motion forces hardly impact on dynamics of the mobile robot, complying with our assumption. The CPU of the robot is an AT89C52 microprocessor running at 24 MHz, and DC motors with LM629 motion controllers are mounted on the driving wheels. The LM629 chip is used as a velocity controller which receives only a reference velocity as the input signal and implicitly produces torque according to the reference velocity via the L298 driver chip. Such a feature of LM629 makes it impossible to access torque directly in the control procedure. Therefore, in the experiments we generated control inputs as velocity terms by integrating $\mathbf{u}$ from (15). The maximum speed of the robot is about 1.46 m/sec.

The perspective view of the robot system with the vision system, the host computer, the communication system and the pitch is shown in Fig. 4. The vision system estimates the posture information of the robot and transmits it to the host computer. It consists of a TMC-7 CCD camera with the resolution of 320×240 pixels and a Dooin Multimedia 7 image grabber with the processing rate of 30 frames/sec. Since the localization of the robot is made only by the vision system, the processing rate of the vision system limits the sampling time for the controller. In the experiments the sampling time

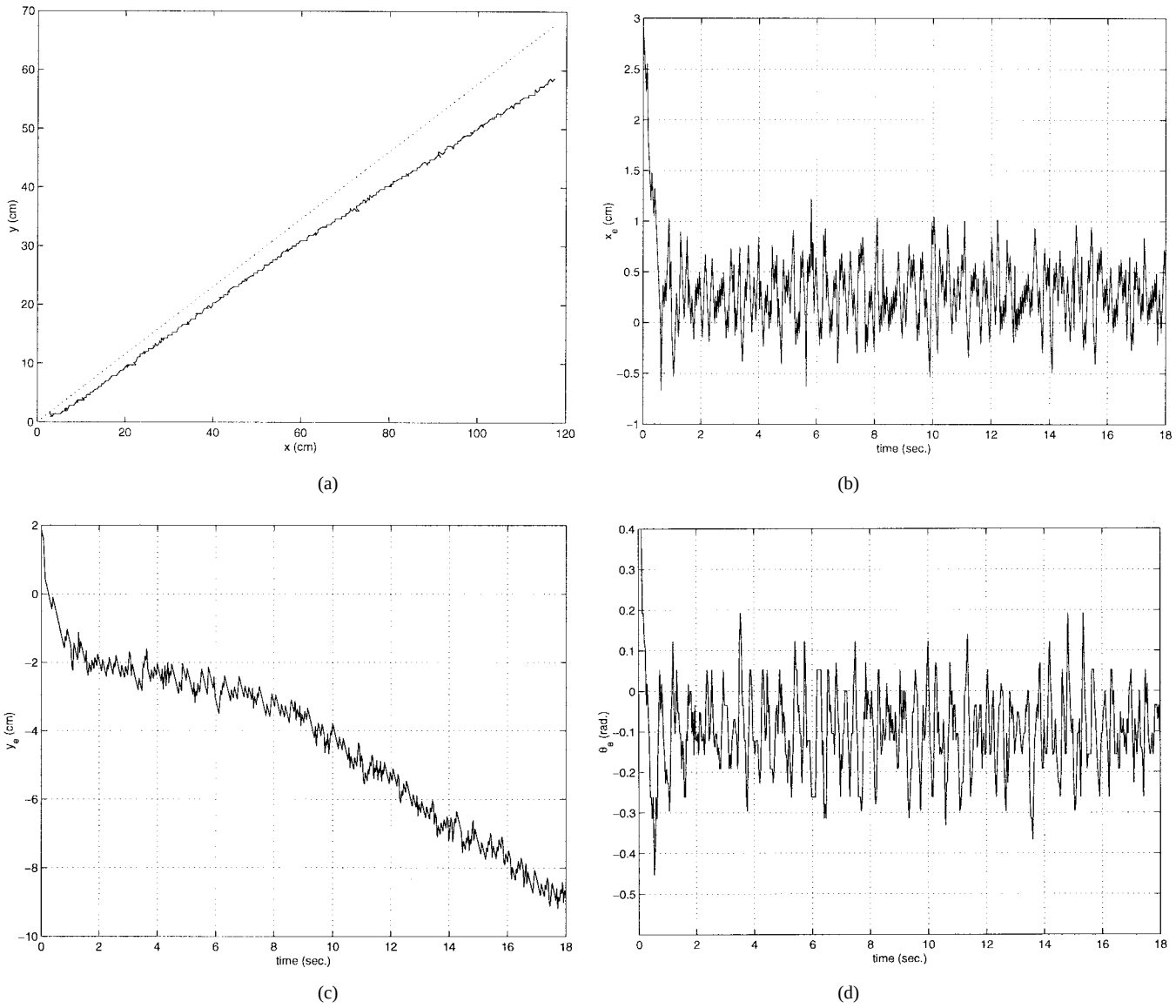

Fig. 9. Straight-line motion using the ϵ-tracking controller with initial errors of (2.43 cm, 3.08 cm, -0.96 radian): (a) x-y plot (dotted line is the reference trajectory), (b) x_e, (c) y_e and (d) θ_e.

is set to be 33 ms, which is identical to the processing rate. The host computer is a Pentium processor with 133 MHz. Control commands are generated from the host computer and sent to the robot through the communication system, which is a RF (Radio Frequency) module running at the speed of 9600 bps. The software for implementing the control algorithm was developed in Visual C++ 1.5 programming language. The experiments were carried out on the MiroSot pitch [21], of which size is 130 cm $\times$ 90 cm.

Fig. 5 is the schematic diagram of the robot control system. While there exist known or unknown external disturbances in the hardware of the control system, we focused our concern on the following disturbances in the experiments.

1) Integration error: As shown in Fig. 5, control inputs should be transformed by an integrator into velocity values for the LM629 motion controller. In this process, intrinsic errors from integration lead to perturbation of the control input $\mathbf{u}$.
2) Noise in control signal: The control commands are sent to the mobile robot as the RF signal, which is inevitably contaminated with added noises from outer environment. In the experiments, the upper bounds of the noises were set heuristically.

In addition to these, it is noted that there exist disturbances in signals of the posture information from the vision system. As was mentioned above, the position and orientation of the robot are estimated only visually without any dead-reckoning capability. Therefore, there are measurement errors in the posture data which stem from the time delay of the vision system or inaccuracy of its processed images. Indeed, the vision system in the experimental setup has measurement errors of about 2.40 cm for position and 4.83 degree for orientation. The upper bound of the measurement error in assumption ii) in the previous section is thus $\rho_f = 2.40$ cm.

B. Experimental Results

In order to validate the applicability of the proposed control scheme, the mobile robot was required to track reference trajectories. Two kinds of reference trajectory, straight-line and curve motion, were planned. As will be shown later, reference trajectories of the mobile robot were generated by a path planner in the frame of the X-Y coordinates, which is often the case. In the experiments, for using the proposed control scheme, reference trajectories were transformed into polar coordinates before generating control commands.

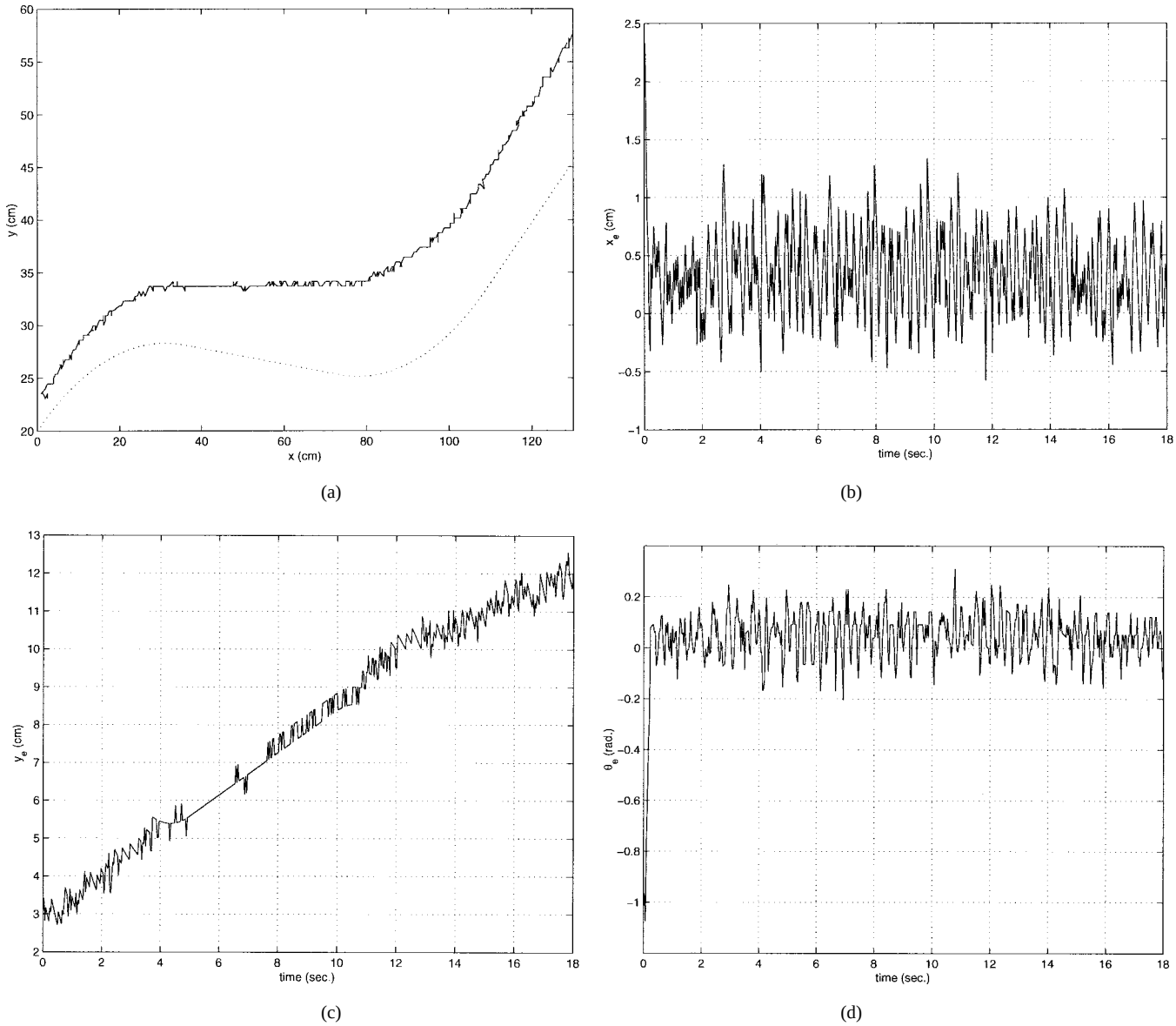

Fig. 10. Curve motion using the ϵ-tracking controller with initial errors of (2.92 cm, 1.85 cm, 0.56 radian): (a) x-y plot (dotted line is the reference trajectory), (b) x_e, (c) y_e and (d) θ_e.

The experimental results for the straight-line tracking are shown in Figs. 6 and 7. Fig. 6 is the result where there were relatively small initial posture errors of 7.09 cm, 1.72 cm and -0.38 radian for x_e, y_e and θ_e, respectively. Fig. 7 is the result in which the robot started tracking with large initial errors of 52.58 cm, 16.62 cm and -3.09 radian. As we can see, the mobile robot eventually approached the reference trajectory with asymptotic stability. In particular, as shown in Fig. 7(a), if the robot was located with large initial posture errors, there was a time of transition in which the tracking error of heading direction was stabilized through forward and backward motion of the robot. Such a motion ascribes to the constraint of the robot's trajectory that the heading direction should not be tangential of a circle around the origin of the world coordinates. Fig. 8 is the result of the curve tracking with initial errors of 11.20 cm, 28.92 cm and -1.31 radian for x_e, y_e and θ_e, respectively. Although there were forward and backward fluctuations initially in the X direction like the case of the straight-line motion, all the three posture variables converged to desired trajectories. It is confirmed that the proposed sliding mode control law was successfully used for the purpose of trajectory tracking of the nonholonomic mobile robot in the presence of external disturbances.

For a comparison purpose, a sliding mode controller for trajectory tracking of nonholonomic mobile robots [10] was also implemented and tested under the same condition. The controller from [10] is referred as the "ϵ-tracking controller" from the fact that for any $\epsilon > 0$ it could make the controlled systems converge to the ϵ-vicinity of reference trajectories in a finite time theoretically. The real trajectories on the X-Y plane and the tracking errors with respect to position and orientation are shown in Figs. 9 and 10. They show that in both motions the mobile robot failed to converge to the reference trajectory, in particular, in the Y direction. This indicates that the ϵ-tracking controller was unable to achieve robustness against the external disturbances existing in the robot system, resulting in only partially stabilized behaviors. Moreover, the chattering behavior in the actual trajectories higher than the case of the proposed controller demonstrates the superior behavior of the proposed controller in response to the use of the switching function.

VI. Conclusion

A novel control algorithm to achieve trajectory tracking of a mobile robot with nonholonomic constraints was proposed. The proposed control scheme uses the computed-torque method for feedback-linearization of the dynamic equation and a theory of sliding mode for robust control. The major contributions of this paper lie in the establishment of a new tracking control scheme for a mobile robot with two control inputs to asymptotically stabilize to a desired trajectory consisting of three posture variables. In particular, the proposed control scheme has the ability to solve the trajectory tracking problem based on dynamic modeling when the reference trajectory is not given as a closed-form. This problem was being unsolved until now in the class of application of sliding mode control algorithm for nonholonomic systems. It was shown that, by applying the sliding mode control, the controlled behavior of a mobile robot is robust against initial condition errors and external disturbances such as integration error, noise in control signal, localization errors, etc. The proposed algorithm was implemented on a vision-based mobile robot system. The experimental comparative results with a previous scheme shows the superiority of our approach in tracking capability and robustness in the presence of such uncertainties as mentioned above.

We conclude this paper by providing two topics for further research.

1) As we can know from assumption 3) in Section IV, there is a prohibitive behavior in robot motion that it should not have a posture whose heading direction is tangential of any circle drawn around the origin of the world coordinates. This constraint causes restriction in planning feasible paths for the robot in some environments. Therefore, an improvement in performance of the control scheme should be necessary for eliminating such a constraint.
2) As a matter of fact, there is a technical difficulty in design of robust controllers for nonholonomic systems with model uncertainties. It is because inherently the number of control inputs is always less than that of state variables in dynamics of nonholonomic systems. Development of a general scheme for dealing with uncertainties in dynamics of nonholonomic systems is a challenging topic for further research.

References

[1] R. W. Brockett, "Asymptotic stability and feedback stabilization," in *Differential Geometric Control Theory*, R. W. Brockett, R. S. Millman, and H. J. Sussmann, Eds. Boston, MA: Birkhauser, 1983, pp. 181–191.

[2] I. Kolmanovsky and N. H. McClamroch, "Developments in nonholonomic control problems," *IEEE Contr. Syst. Mag.*, vol. 15, pp. 20–36, Dec. 1995.

[3] Z. P. Jiang and J.-B. Pomet, "Combining backstepping and time-varying techniques for a new set of adaptive controllers," in *Proc. IEEE Int. Conf. Decision Contr.*, Dec. 1994, pp. 2207–2212.

[4] Z. P. Jiang, "Iterative design of time-varying stabilizers for multi-input systems in chained form," *Syst. Contr. Lett.*, vol. 28, pp. 255–262, 1996.

[5] T. Hamel and D. Meizel, "Robust control laws for wheeled mobile robots," *Int. J. Syst. Sci.*, vol. 27, no. 8, pp. 695–704, 1996.

[6] L. E. Aguilar, P. Souères, M. Courdesses, and S. Fleury, "Robust path-following control with exponential stability for mobile robots," in *Proc. IEEE Int. Conf. Robot. Automat.*, May 1998, pp. 3279–3284.

[7] J. J. E. Slotine and S. S. Sastry, "Tracking control of nonlinear systems using sliding surfaces, with application to robot manipulators," *Int. J. Contr.*, vol. 38, no. 2, pp. 465–492, 1983.

[8] K. S. Yeung and Y. P. Chen, "A new controller design for manipulators using the theory of variable structure systems," *IEEE Trans. Automat. Contr.*, vol. 33, pp. 200–206, Feb. 1988.

[9] A. Bloch and S. Drakunov, "Stabilization of a nonholonomic system via sliding modes," in *Proc. IEEE Int. Conf. Decision Contr.*, Dec. 1994, pp. 2961–2963.

[10] ____, "Tracking in nonholonomic dynamic systems via sliding modes," in *Proc. IEEE Int. Conf. Decision Contr.*, Dec. 1995, pp. 2103–2106.

[11] J. Guldner and V. I. Utkin, "Stabilization of nonholonomic mobile robots using Lyapunov functions for navigation and sliding mode control," in *Proc. IEEE Int. Conf. Decision Contr.*, Dec. 1994, pp. 2967–2972.

[12] ____, "Sliding mode control for gradient tracking and robot navigation using artificial potential fields," *IEEE Trans. Robot. Automat.*, vol. 11, pp. 247–254, Apr. 1995.

[13] J. A. Chacal B. and H. Sira-Ramirez, "On the sliding mode control of wheeled mobile robots," in *Proc. IEEE Int. Conf. Syst. Man. Cybern.*, Sept. 1994, pp. 1938–1943.

[14] L. E. Aguilar, T. Hamel, and P. Soueres, "Robust path following control for wheeled robots via sliding mode techniques," in *Proc. 1997 IEEE/RSJ Int. Conf. Intell. Robot. Syst. (IROS'97)*, Sept. 1997, pp. 1389–1395.

[15] C.-Y. Su and Y. Stepanenko, "Robust motion/force control of mechanical systems with classical nonholonomic constraints," *IEEE Trans. Automat. Contr.*, vol. 39, pp. 609–614, Mar. 1994.

[16] H.-S. Shim, J.-H. Kim, and K. Koh, "Variable structure control of nonholonomic wheeled mobile robots," in *Proc. IEEE Int. Conf. Robot. Automat.*, May 1995, pp. 1694–1699.

[17] B. D'Andréa-Novel, G. Bastin, and G. Campion, "Dynamic feedback linearization of nonholonomic wheeled mobile robots," in *Proc. IEEE Int. Conf. Robot. Automat.*, 1992, pp. 2527–2532.

[18] F. L. Lewis, C. T. Abdallah, and D. M. Dawson, *Control of Robot Manipulators*. New York: Macmillan, 1993.

[19] M. Aicardi, G. Casalino, A. Bicchi, and A. Balestrino, "Closed loop steering of unicycle-like vehicles via Lyapunov techniques," *IEEE Robot. Automat. Mag.*, vol. 2, pp. 27–35, Mar. 1995.

[20] W. Gao and J. C. Hung, "Variable structure control of nonlinear systems: A new approach," *IEEE Trans. Ind. Electron.*, vol. 40, pp. 44–55, Feb. 1993.

[21] J.-H. Kim, H.-S. Shim, H.-S. Kim, M.-J. Jung, I.-H. Choi, and J.-O. Kim, "A cooperative multi-agent system and its real time application to robot soccer," in *Proc. IEEE Int. Conf. Robot. Automat.*, Apr. 1997, pp. 638–643.

[22] J.-H. Kim, Ed., *Robotics and Autonomous Systems*, Special Issue: First Micro-Robot World Cup Soccer Tournament, MiroSot, vol. 21, no. 2, Sept. 1997.